journal

J. Am. Ceram. Soc., 74 [11] 2776–80 (1991)

Cracking and Damage in a Notched Unidirectional Fiber-Reinforced Brittle Matrix Composite

Rajendra K. Bordia*

Experimental Station, Central Research and Development Department, E. I. du Pont de Nemours & Company, Inc., Wilmington, Delaware 19880

Brian J. Dalgleish,*,* Panos G. Charalambides,*,† and Anthony G. Evans*

Materials Department, College of Engineering, University of California, Santa Barbara, California 93106

Results of four-point bend tests on notched beams of a laminated unidirectional fiber-reinforced glass matrix composite are presented. The failure sequence has been established through in situ examination. The dominant damage mode is a mixed-mode, split crack that runs parallel to the predominant fiber directions. The crack interacts with and crosses over imperfectly aligned fibers. The resulting bridging tractions are sufficient to cause the critical strain energy release rate to increase substantially as the crack extends. Several other damage modes are also observed. These include mode I (tensile) matrix cracks bridged by fibers, mode II (shear) cracks, and compressive damage at the loading points. [Key words: bending, failure, fibers, composites, cracks.]

I. Introduction

Anisotropic fibrous composites are susceptible to cracking on planes parallel to the loading axis[1–5] when tested in the presence of holes and notches (Fig. 1). These split cracks are either mixed mode or mode II, depending on the configuration and the placement of the notch.[6–9] Such cracking has the attribute that the composite is rendered notch insensitive.[10] However, this benefit is usually counteracted by various detrimental effects, such as reduced stiffness and degraded transverse strength. Consequently, it is important to understand the process that governs mixed-mode, split cracking and to identify microstructural means for suppressing it. The present study addresses this issue. Cracks of the type depicted in Fig. 1 have several manifestations. They occur in wood upon monotonic loading[1] and in laminated polymer matrix composites upon cyclic loading.[3] They have also been noted in laminated ceramic matrix composites, both in unidirectional material and in 0/90 laminates.[2,4,5,10] The most comprehensive study of this phenomenon has been on a 0/90 laminate LAS matrix composite reinforced with Nicalon‡ fiber.[2] The present study emphasizes this mode of cracking in a laminated unidirectional ceramic matrix composite.

In the above studies, an analysis of the energy release rate $\mathcal{G}$ with crack length a was used, which indicated that $\mathcal{G}$ has the general characteristic depicted in Fig. 1.[11] Notably, a steady-state, $\mathcal{G}_{SS}$ is reached after the split crack has exceeded a length $a \gg h_0$ (the notch depth). Furthermore, for notched beams in four-point flexure, the steady-state strain energy release rate is[7,8] given by

$$\mathcal{G}_{SS} = \frac{6M^2(1 - \nu_{12}\nu_{21})}{E_{11}}\left[\frac{1}{(h - h_0)^3} - \frac{1}{h^3}\right] \quad (1)$$

where M is the bending moment per unit width, E_{11} is the longitudinal modulus, h is the beam thickness (Fig. 1), ν_{12} and ν_{21} are the Poisson's ratios (defined such that $\nu_{ij} = \epsilon_i/\epsilon_j$ due to an applied normal stress σ_{ij}, with ϵ_i and ϵ_j being the normal strains in the mutually orthogonal i and j directions).

Based on these energy release rates, the mixed-mode fracture resistance $\mathcal{G}_R$ for the 0/90 laminated lithium aluminum silicate (LAS) matrix composite was found to increase with crack length, commencing with a value, $\mathcal{G}_0 = \Gamma_m$, the matrix fracture energy. Observation of the crack trajectory revealed that the cracks were located in the 0° layer near the 0/90 interface. However, because the fibers were imperfectly aligned, the crack intersected and crossed over some of the fibers. These intact fibers were observed to bridge the crack surface and resist crack opening.[2,12] A subsequent simulation of this behavior[12] indicated that the increase in resistance depended both on the magnitude of the *forces p* exerted by the fibers and on the sensitivity of *matrix fracture* to shear. The effect of shear on the matrix fracture energy Γ_m is manifest in a parameter λ, defined as[13]

$$\Gamma_m = \Gamma_0[1 - (1 - \lambda)\sin^2\Psi]^{-1} \quad (2)$$

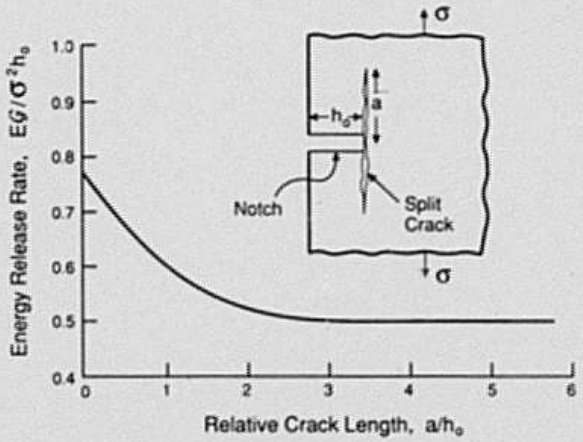

Fig. 1. Schematic indicating split cracks formed from a notch and trends in the energy release rate.

J. J. Brennan—contributing editor

Manuscript No. 197325. Received August 27, 1990; approved June 21, 1991.

*Member, American Ceramic Society.

*Present address: Lawrence Berkeley Laboratories, Berkeley, CA.

†Present address: Department of Mechanical Engineering and Engineering Mechanics, Michigan Technological University, Houghton, MI 49931.

‡Nippon Carbon, Tokyo, Japan.

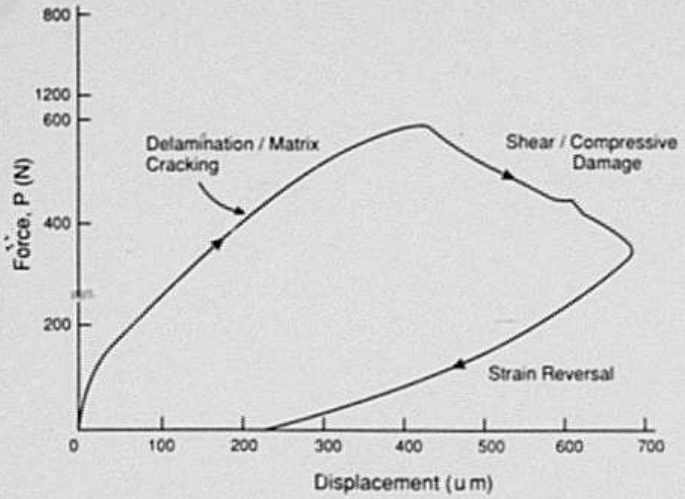

Fig. 2. Typical load–displacement curve for notched beams tested in four-point flexure.

where Ψ is the phase angle of loading[‡] and Γ_0 is the mode I ($\Psi = 0$) *matrix* fracture energy. The parameter λ is found to be about 0.3 for various brittle systems, indicative of a significant shielding of the shear mode during mixed-mode fracture.[13] An important emphasis of the present study is thus on interactions between split cracks and fibers and the ensuing influence of bridging fibers on the propagation resistance of the cracks, $\mathcal{G}_R$, through the parameters, p, and λ.

II. Experimental Procedure

This study was conducted on a unidirectional Nicalon fiber-reinforced laminated composite with a *borosilicate* glass matrix.[¶] The fiber volume fraction was $f \approx 0.45$. The material was prepared by hot-pressing.[14] Beams of approximate dimensions 3 mm × 6 mm × 45 mm were machined from plates such that the fiber and beam axes were coincident. On most beams, notches were introduced using diamond blades. The width and the depth of the notches were 0.5 mm and 2 mm, respectively. The tensile face and one side surface of the beams were polished, using diamond polishing media, as needed, to observe cracking and damage in either optical or scanning electron microscopes.

Four-point flexure tests were performed using a constant load point displacement rate of 0.85 μm/s. The midpoint deflection, u, was monitored on the tensile face. Friction was minimized by using a thin layer of solid lubricant between the sample and the load points.[9] Specimens were monotonically loaded and the crosshead was periodically arrested in order to measure the delamination crack length using a low-magnification, long focal length microscope. In other experiments, samples were unloaded, as needed, to measure the hysteresis and to observe cracking and damage at higher magnifications. Finally, a few experiments were conducted in situ on an optical microscope.

Several unnotched beams were also tested in four-point flexure. Results from these tests were used to estimate the modulus, the matrix cracking stress, and the interfacial sliding stress.

III. Results

(I) *Mechanical Measurements*

Load–displacement data obtained on unnotched beams have been analyzed in the elastic range to estimate a longitudinal modulus as $E_{11} \approx 115$ GPa. Based on the known modulus of the fibers[4,5] ($E_f \approx 200$ GPa) and the volume fraction ($f = 0.45$), the composite modulus is consistent with a matrix modulus $E_m \approx 50$ GPa. The load at which mode I matrix cracks were first observed to form by in situ observation was used in conjunction with elastic analysis of the beam to indicate a matrix cracking stress, $\sigma_0 = 210 \pm 20$ MPa, consistent with previous measurements.[10,15]

Experiments conducted on *notched beams* gave relations between load and midpoint displacement of the type plotted on Fig. 2. The peak loads attained were about 4 times higher than the load at which the first nonlinearity appeared. The samples also exhibited significant residual displacement. In situ observations (Fig. 3) revealed that a split crack formed and propagated normal to the notch as the load increased. The dependence of the length, a, of the crack on the applied load, P, determined from these observations (Fig. 4) indicated that crack extension occurred with rising load. Furthermore, the crack extension was discontinuous, such that the crack would grow in increments of a few hundred micrometers. This phenomenon is partially responsible for variability in the data between samples. Information concerning the load, P,

[‡]Ψ is defined as $\tan^{-1}(K_{II}/K_I)$, where K_{II} and K_I are the mode II and mode I stress intensity factors, respectively. Hence, $\Psi = 0$ refers to pure opening and $\Psi = \pi/2$ is pure shear.

[¶]Corning 7740, Corning, Inc., Corning, NY.

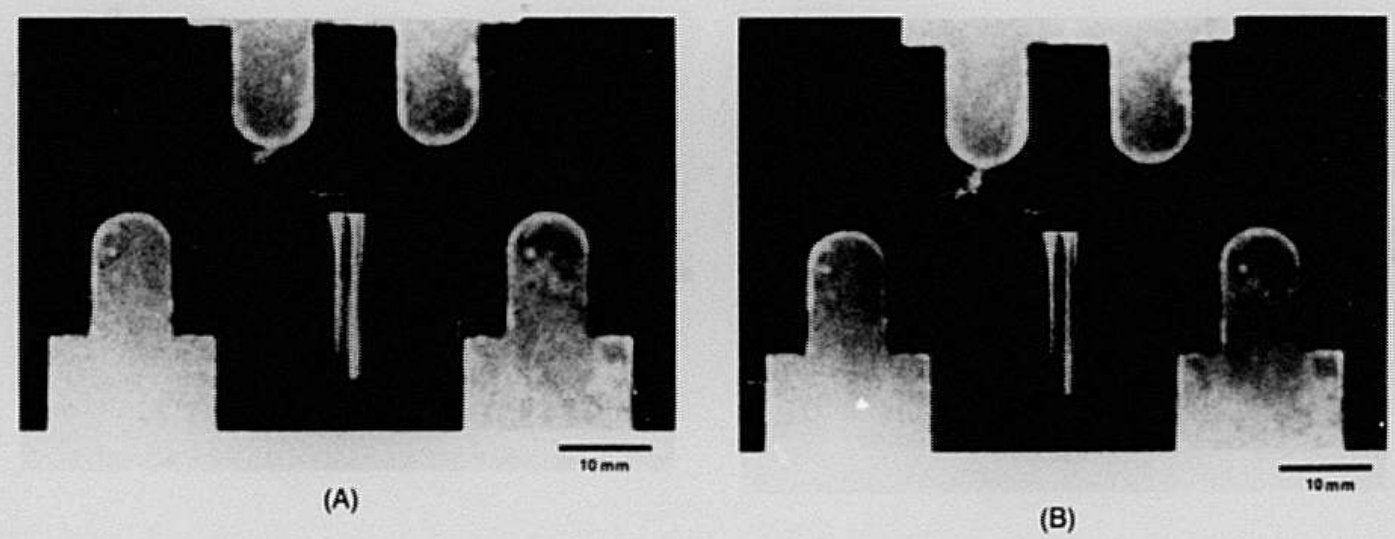

Fig. 3. Low-magnification photographs of the damage during testing: (A) split crack and compressive damage at loading points, load 490 N; (B) mode II (shear) crack has also initiated and coalesced with the compressive damage, load 620 N.

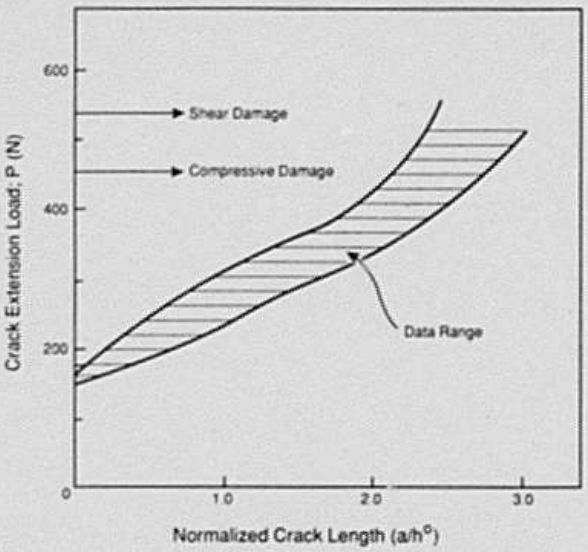

Fig. 4. Crack extension load as a function of the split crack length.

and the length, a, of the split crack can be used in conjunction with Eq. (1) and the specimen dimensions to determine the growth resistance, $\mathcal{G}_R$, subject to the premise that the *beam is linear elastic*. The result is plotted on Fig. 5. Two features are emphasized: (i) The resistance $\mathcal{G}_R$ increases *substantially* as the crack length increases, with no evidence of an asymptote. (ii) The initiation resistance, $\mathcal{G}_0 \approx 120\ \mathrm{J \cdot m^{-2}}$ is much higher than the fracture energy for the borosilicate glass matrix, $\Gamma_0 \approx 10\ \mathrm{J \cdot m^{-2}}$.

(2) Observations of Damage

A summary of the damage modes (Figs. 3 and 6) is presented in a schematic (Fig. 7). The first damage to be observed was a single *mode I matrix crack* which initiates from the vicinity of the notch tip at a load of ~150 N. This crack extended to about the midplane of the net section. This crack was fully bridged by intact fibers. This event was followed by *split cracking perpendicular to the notch*. These cracks were not confined to the matrix, but crossed over fibers, because of the imperfect fiber alignment. The bridging fibers remained intact and pulled out from the matrix, as well as being subject to bending as the cracks extended. The extension of the mixed-mode crack was accompanied by the formation of additional mode I matrix cracks in the net section. These two processes continued for most of the test. The split crack arrested when the crack length was about equal to the inner loading span. At a load of about 450 N, visible compressive damage (crushing) was noted at the loading points. This was followed by formation of shear damage between the inner and the outer loading points. The final failure of the sample occurred by coalescence of the shear and compressive damage. The average loads at which these various damage modes initiated has been indicated on Fig. 4.

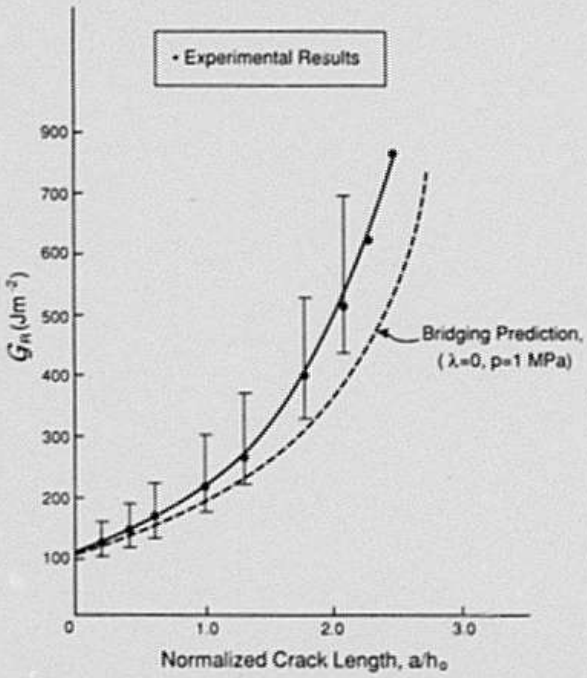

Fig. 5. Nominal resistance, $\mathcal{G}_R$, as a function of the normalized crack length (a/h_0). Also shown is the predicted line based on fiber bridging, with $\lambda = 0$, $p = 1$ MPa, with the origin placed at $\mathcal{G}_0 = 120\ \mathrm{J \cdot m^{-2}}$.

The spacing between the mode I matrix cracks, d, decreased and saturated at $d \approx 230\ \mu\mathrm{m}$. This spacing has been used to estimate the interface sliding stress[15,16] through the expression[15]

$$\tau \approx 1.34[(1 - f^2)\Gamma_0 E_f E_m R^2 / f E_{11} d^3]^{1/2} \tag{3}$$

where R is the fiber radius (~8 μm) and the subscripts f and m refer to fiber and matrix, respectively. Based on Eq. (3), with $\Gamma_0 = 10\ \mathrm{J \cdot m^{-2}}$ for borosilicate glass, the sliding stress is found to be $\tau = 2$ MPa, consistent with other measurements.[15]

IV. Discussion

The splitting resistance, $\mathcal{G}_R$, evaluated *as if the beam were linear* (Fig. 5), is evidently *invalidated* by nonlinearities, manifest in the multiple damage modes. Nevertheless, at loads below that at which either compressive or shear damage initiates, an attempt is made to ascertain the approximate applicability of this representation and to rationalize the magnitudes of the resistance. The misaligned fibers that cross over and bridge the crack are one source of the relatively large $\mathcal{G}_R$ and of the increase in $\mathcal{G}_R$ with crack extension, as in the 0/90 laminate.[2] The mode I matrix cracks that accompany delamination should also *contribute to the resistance*. The latter is addressed first.

Specifically, it can be argued that the in-plane tension beneath the mixed-mode, split crack (Fig. 8) induces mode I matrix cracking and, thus, that such cracking is a *necessary* adjunct to the mixed-mode crack resistance. The frictional dissipation that occurs at the fiber/matrix interfaces upon mode I matrix cracking can then be considered as a component of the mixed-mode, split crack resistance *itself*. A simplified estimate of the dissipation can be derived from the hysteresis in the stress–strain curve upon mode I matrix cracking, given by the ACK model[16] (Fig. 8). The hysteresis ΔU is

$$\Delta U = (\sigma_0^2 / 2E_{11})(E_{11}/fE_f - 1) \tag{4}$$

where σ_0 is the mode I matrix cracking stress. In turn, ΔU is related to the contribution to the steady-state fracture resistance of split cracks given by mode I matrix cracks, $\Delta\Gamma_m$, as

$$\Delta\Gamma_m \approx w\Delta U \tag{5}$$

where w is the width of the matrix crack zone (Fig. 8). Inserting values of the parameters summarized in Table I gives $\Delta\Gamma_m \approx 100\ \mathrm{J \cdot m^{-2}}$. Since the length and spacing of the mode I matrix cracks were observed to be independent of the split crack length, their contribution to the fracture energy, $\Delta\Gamma_m$, should be essentially invariant with the length of the split crack. Hence, to first order, $\Delta\Gamma_m$ may be *subtracted* from the measured split crack resistance. This procedure yields a modified *initiation* resistance $\mathcal{G}_0 \approx 20\ \mathrm{J \cdot m^{-2}}$, similar to the fracture energy for the borosilicate matrix ($\Gamma_0 \approx 10\ \mathrm{J \cdot m^{-2}}$).

The effect of the misaligned fibers on the split crack growth resistance can be addressed by means of a direct fit of

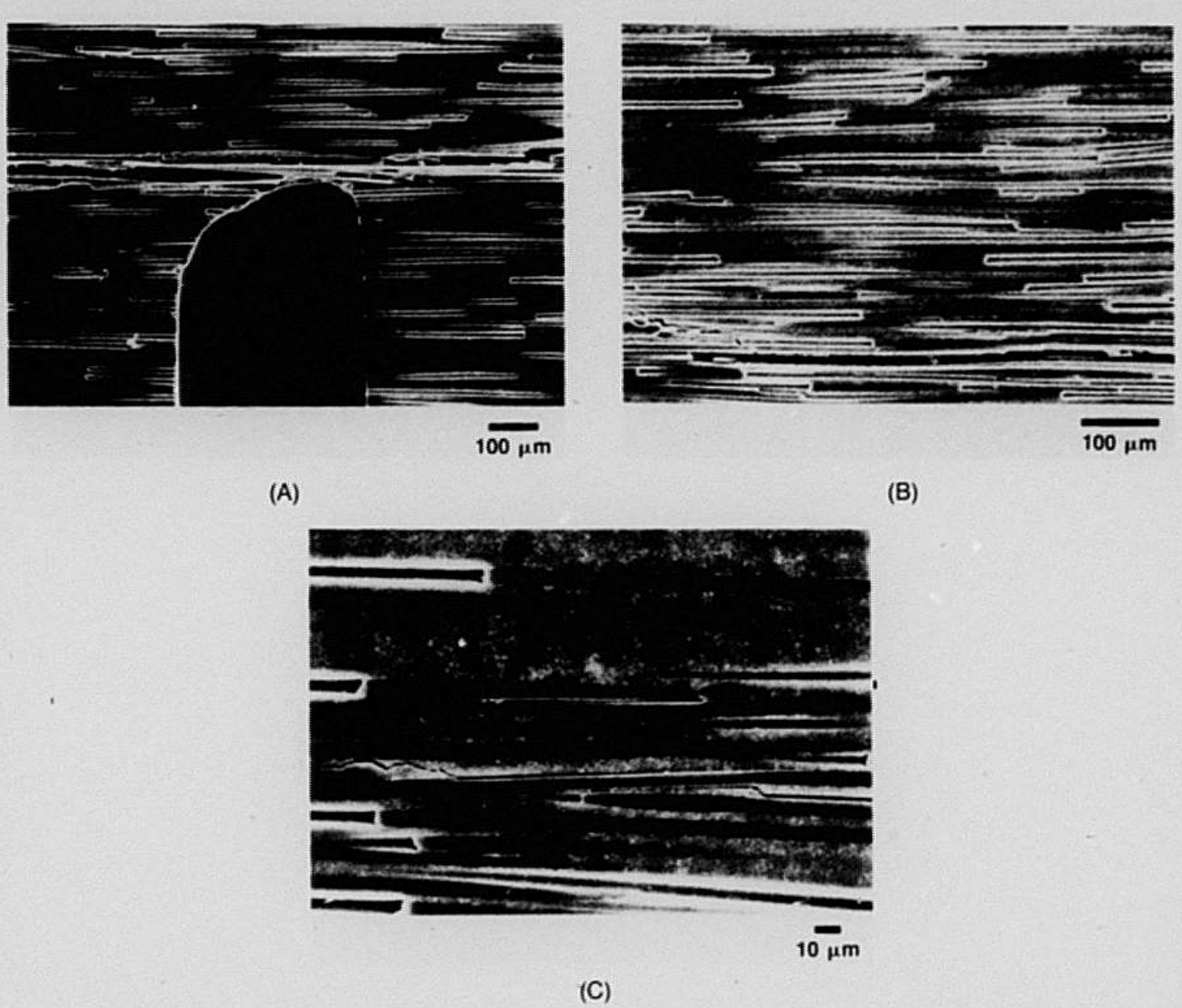

Fig. 6. Scanning electron micrographs from a sample tested to failure: (A) the split crack bridged by intact fibers; (B) and (C) the split crack jumps from one fiber–matrix interface to another. Also note the tensile (mode I) cracks originating from the split crack.

the experimental results to resistance curve simulations based on bridging fibers.[12] Such simulations use the resistance at $a = 0$ as origin and then predict the *increase* in resistance with crack extension caused by the fibers. The simulated curve that provides best agreement with the data, starting at $\mathcal{G}_0 = 120\ \mathrm{J \cdot m^{-2}}$, is shown in Fig. 5. This curve has a mixity parameter $\lambda = 0$ and traction caused by the bridging fibers, $p = 1$ MPa. Given the extreme nonplanarity of the matrix crack (Fig. 7) and the tendency for nonplanarity to reduce λ toward zero,[17] the inferred λ appears to be reasonable. Furthermore, the order of magnitude of the crack surface tractions $p = 1$ MPa is similar to the sliding stress $\tau \approx 2$ MPa

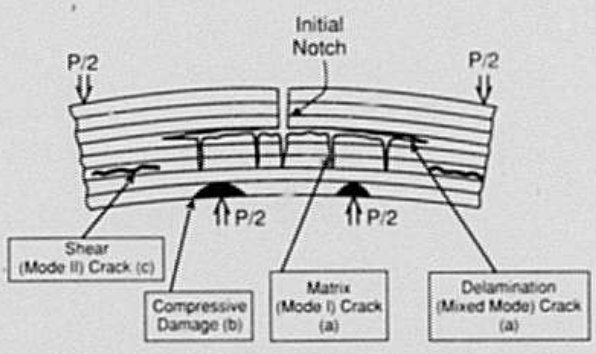

Fig. 7. Schematic of the various damage modes observed and their initiation sequence (damage modes labeled (a) were observed at the lowest loads and (c) at the highest load).

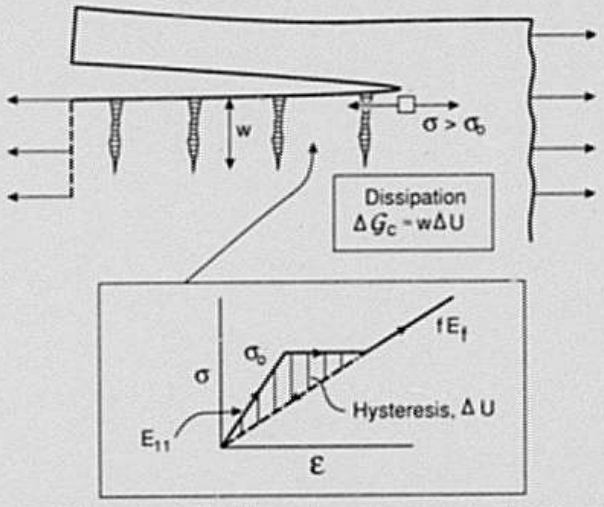

Fig. 8. Schematic of the effects of matrix cracks on the split crack growth resistance.

Table I. Summary of Composite Properties

Property	Value
Matrix cracking stress, σ_o	210 MPa
Sliding stress, τ	2 MPa
Longitudinal modulus, E_{11}	115 GPa
Fiber modulus, E_f	200 GPa
Fiber volume fraction, f	0.46
Width of matrix crack zone, W	2 mm

and, again, appears reasonable, given that fiber pullout is observed to accompany crack growth.

V. Concluding Remarks

Various damage modes that accompany the testing of notched, unidirectionally reinforced laminated glass matrix composites have been identified. Emphasis has been placed on the progression of mixed-mode split cracks from the base of the notch. The extension of such cracks is found to involve appreciably larger energy release rates $\mathcal{G}_R$ than the analogous process in [0/90] laminated LAS matrix composites.[2] The large $\mathcal{G}_R$ and its dependence on the crack length have been attributed primarily to a crack path that intercepts misaligned fibers, leading to a substantial fiber bridging resistance. In addition, the growth of the split crack is accompanied by mode I matrix cracks. This additional cracking was not observed in the laminated [0/90] composites studied previously.[2] The large effect of bridging fibers on $\mathcal{G}_R$ is consistent with previous predictions[12] and suggests fiber architecture concepts that incorporate a relatively small volume fraction of fibers that are either misaligned or thread across prospective delamination planes.

Acknowledgment: We thank Dr. D. B. Marshall for his assistance in conducting the in situ experiments.

References

[1]M. F. Ashby, K. E. Easterling, R. Harrysson, and S. K. Maiti, *Proc. R. Soc. London, A*, **4398**, 24 (1985).
[2]O. Sbaizero, P. G. Charalambides, and A. G. Evans, "Delamination Cracking in a Laminated Ceramic-Matrix Composite," *J. Am. Ceram. Soc.*, **73** [7] 1936–40 (1990).
[3]M. Spearing, P. W. R. Beaumont, and M. F. Ashby, *Composite Materials; Fatigue and Fracture*, ASTM STP 1110. Edited by T. K. O'Brien. In press.
[4]K. M. Prewo, "Development of Fiber Reinforced Glasses and Glass-Ceramics"; pp. 529–47 in Materials Science Research, Vol. 20, *Tailoring Multiphase and Composite Mechanics*. Edited by R. E. Tressler, C. c. Messing, C. G. Pantano, and R. E. Newnham. Plenum Press, New York, 1986.
[5]J. J. Brennan and K. M. Prewo, "Silicon Carbide Fiber Reinforced Glass-Ceramic Matrix Composites Exhibiting High Strength and Toughness," *J. Mater. Sci.*, **17**, 2371–83 (1982).
[6]Z. Suo, "Delamination Specimens for Orthotropic Material," Report No., Mech 135. Harvard University, Cambridge, MA, 1989.
[7]P. G. Charalambides, J. Lund, A. G. Evans, and R. M. McMeeking, "A Test Specimen for Determining the Fracture Resistance of Bimaterial Interfaces," *J. Appl. Mech.*, **111**, 77–82 (1989).
[8]P. G. Charalambides, "Some Anisotropic Aspects and the Analysis of Mixed Mode Delamination Cracking in Fiber Reinforced and Laminated Ceramic Matrix Composites"; unpublished work.
[9]P. G. Charalambides, H. C. Cao, J. Lund, and A. G. Evans, "A Test Specimen for Determining the Fracture Resistance of Bimaterial Interfaces," *Mech. Mater.*, **8**, 269 (1990).
[10]A. G. Evans and D. B. Marshall, "The Mechanical Behavior of Ceramic Matrix Composites," *Acta Metall.*, **37**, 2567 (1989).
[11]M. D. Thouless, H. C. Cao, and P. A. Mataga, "The Decohesion of Thin Films," *J. Mater. Sci.*, **24**, 1406 (1989).
[12]G. Bao, B. Fan, and A. G. Evans, "Mixed Mode Delamination Cracking in Composites," *Mech. Mater.*, in press.
[13]H. Jensen, J. W. Hutchinson, and K. S. Kim, "Decohesion of a Cut Prestressed Film," *Int. J. Solids Struct.*, **20**, 1099 (1990).
[14]K. M. Prewo and J. J. Brennan, "Silicon Carbide Yarn Reinforced Glass Matrix Composites," *J. Mater. Sci.*, **17**, 1201 (1982).
[15]H. C. Cao, E. Bischoff, O. Sbaizero, M. Rühle, A. G. Evans, D. B. Marshall, and J. J. Brennan, "Effect of Interfaces on the Properties of Reinforced Ceramics," *J. Am. Ceram. Soc.*, **73** [6] 169–99 (1990).
[16]J. Aveston, G. A. Cooper, and A. Kelly, "Single and Multiple Fracture"; pp. 15–26 in *Properties of Fiber Composites*, Conference Proceedings of the National Physical Laboratories. IPC Science and Technology Press Ltd., Surrey, U.K., 1971.
[17]A. G. Evans and J. W. Hutchinson, "Effects of Non-Planarity on the Fracture Resistance of Interfaces," *Acta Metall.*, **37**, 909 (1989). □